Journal of Zhejiang University-SCIENCE A (Applied Physics & Engineering)
ISSN 1673-565X (Print); ISSN 1862-1775 (Online)
www.zju.edu.cn/jzus; www.springerlink.com
E-mail: jzus@zju.edu.cn

Comparative study of static and dynamic parameters of rock for the Xishan Rock Cliff Statue

Jin JIANG[†1], Jin-zhong SUN[2]

([1]*School of Civil and Environmental Engineering, Nanyang Technological University, 639798, Singapore*)

([2]*School of Engineering and Technology, China University of Geosciences, Beijing 100083, China*)

[†]E-mail: jian0048@e.ntu.edu.sg

Received Jan. 10, 2011; Revision accepted Mar. 28, 2011; Crosschecked Sept. 7, 2011

Abstract: Ultrasonic wave testing was applied to investigate the quality and weathering status of rock specimens obtained in two borings situated in the Xishan Buddha rock slope in Taiyuan, China. This paper pays special attention to the distribution of bulk density, dynamic parameters and static parameters of rock specimens as well as the relationship between static and dynamic parameters. The results illustrate that the distribution of both parameters is identical along the depth of two drilled holes in the rock slope. When the hole depth increases, the density of rock mass, saturated compression strength and static elastic modulus, dynamic elastic modulus and wave velocity also show increase tendency. The weathering degree in the rock mass ranging from the surface of cliff to the depth of 2.5 m is the highest while the rock mass is unsalted and more rigid when the depth is larger than 3.0 m. The relationship between dynamic elastic modulus, sonic wave velocity and horizontal depth indicates that dynamic elastic modulus is more sensitive than sonic wave velocity. Conversely, by comparing quantity relationship between static elastic modulus and sonic wave velocity, it is found that the composition of rock has a great influence on the relationship between static and dynamic parameters, that is, inequality of rock composition will lead to dispersion and abnormality of the distribution of static and dynamic parameters.

Key words: Xishan Buddha, Rock mechanics, Rock quality, Elastic wave velocity, Elastic modulus, Compression strength, Ultrasonic wave testing

doi:10.1631/jzus.A1100003 **Document code:** A **CLC number:** TU458

1 Introduction

China is one of the civilized countries having a long history and many cultural relics. Some of them exist in the form of rock as cave temples, cliff statues, rock engravings, rock paintings, stone pagodas, stone bridges, stone valves, stone arch of celebrities, rock tombs, etc. In recent years, influenced by weathering, earthquakes and man-made destruction, many precious relics were seriously eroded. Therefore, it is significant and meaningful to investigate the quality of these stone relics to evaluate the state of these civilization heritages and to provide a basis for future protection.

Ultrasonic wave testing is an effective technique by determining rock elastic wave velocity and other parameters in the process of wave propagation in the rock mass to examine the quality of the rock mass and quality variation in spatiality. Mao *et al.* (2005) mentioned that the ultrasonic wave detection technology has been widely used in hydropower construction, railway, and civil engineering, such as in the rock weathering division, rock mass quality analysis and rock dynamic parameters investigation and strength evaluation of concrete structures, etc. In comparison with other mechanical test methods, acoustic measurement technique is simple, fast, and economical. Therefore, it is a powerful tool in examination for the quality of rock mass.

Khan and Irani (1987) described an experimental technique for determination of dynamic tensile fracture strength of brittle solids. In their study, this

technique was applied to determine the dynamic tensile fracture strength of granite, limestone, and sandstone. The specimens were cored perpendicular to the bedding plane for these rocks. The quasi-static fracture strengths of the same solids were also determined for comparison with the dynamic strengths. The dynamic strengths have been found to be several times the quasi-static strengths, thus showing a strong dependence of fracture strength on strain rate. Homand *et al.* (1993) undertook ultrasonic measurements to determine the main structural axes of slate. The dynamic modulus of elasticity was calculated using this method. The confining pressure had a definite influence on Young's modulus, measured at right-angles to the schistosity. Li and Wu (1995) investigated the distribution of elastic parameters and wave velocities in two axes of rock mass in the Longmen Grottoes area and mentioned that the rock mass should be seen as orthotropic for mechanical properties. Guyer *et al.* (1997) established a relationship between static and dynamic modulus with the rock density. It was concluded that density can make a quantitative prediction of dynamic elastics properties. Zhu (1999) investigated the distribution of elastic wave velocity according to the ultrasonic wave testing results in rock mass and influence factors of propagation velocity of elastic wave. Zhao (1999) verified the characteristics of acoustic wave propagation of micro-cracked rock and fractured rock mass under loading or unloading processes by experiments and numerical analysis.

Camborde *et al.* (2000) used the discrete element method to model both the dynamic and non-linear behavior of rocks. Compact and isotropic synthetic media were generated automatically and were used to investigate the mechanical behavior of these low-porosity materials. Deng *et al.* (2000) and Sun (2001) examined the ultrasonic wave velocity of both dry and saturated marbles and found that the wave velocity in saturated marbles is lower than that of dry ones. It was also demonstrated that ultrasonic wave velocity would show great dispersion for saturated specimens and anisotropy was also weakened after long-term immersion in water for marbles. Ravazzoli *et al.* (2003) investigated the acoustic and mechanical properties of saturated reservoir sandstone. The dry-rock moduli were obtained from laboratory measurements for variable confining pressures. The ultrasonic phase velocities and quality factors for different saturations and pore-fluid pressures ranging from normal to abnormally high values were obtained to relate the seismic and ultrasonic velocity and attenuation to the micro structural properties and pressure conditions of the reservoir. Bhasin and Kaynia (2004) performed static and dynamic rock slope stability analyses using a numerical discontinuum modelling technique for a 700-m high rock slope in western Norway. First, an initial static loading was applied in the numerical model to simulate the prevailing rock mass conditions at the site. Second, saturated and weathered joint conditions were modeled by reducing the residual friction angle along the discontinuities of the rock mass. Xu and Wang (2004) analyzed the cause factors for the difference between results obtained by ultrasonic acoustic testing and other methods and investigated the relationship between wave propagation direction and the combination of rock structure surfaces. Wiercigroch *et al.* (2005) evaluated the dynamics of ultrasonic percussive drilling of hard rocks. Jiang (2008) applied both static test results for rock specimens and ultrasonic wave methods to evaluate the stability of rock slope.

In a summary, two methods for measuring the elastic parameters of rocks can now be found. One is to measure the longitudinal and lateral stains of the rock sample under static load, and then to compute the static elasticity parameters of the rock. The other is to measure the longitudinal or transverse wave velocity of the rock and then to calculate the dynamic elasticity parameters by the theory of elastic waves. The ultrasonic method is a non-destructive method so that it is usually used in geotechnical exploration. However, until now, few scholars have investigated the instinctive relationship between the static and dynamic parameters of the sandstone, and this paper especially focuses on this topic.

2 Principle and setup of testing

The fact that wave propagation relies on the density of the medium and elastic modulus is the theoretical basis for the use of wave propagation to study rock properties. Additionally, mass density is one basic indicator of material composition and is in accordance with general physical laws. Variation in material density will lead to alteration of material

mechanical properties. Rock is a product of geological evolvement of the earth so that it has various material compositions and structures, causing complex performance in engineering mechanics. Also density is a comprehensive reflection of micro composition and structure of rock mass. The mechanical properties of rock mass under different loadings have significant meanings to engineering design. According to action mode, force applied on rock mass can be divided into static load and dynamic load. Under different loadings, the rock mass can show different mechanical properties. Under static loading, constitutive model and compressive strength are two main considerations in the process of quality evaluation for rock mass. The parameters describing these two aspects include deformation modulus and Poisson's ratio, etc. When dynamic loading is applied on rock mass, dynamic constitutive model, the dynamic strength and vibration characteristics are mainly focused. It has been recognized by many scholars (Feng, 1988; Bray and Repetto, 1994; Ling and Cheng, 1997; Zhou *et al.*, 2002) that the dynamic properties such as dynamic deformation modulus, dynamic Poisson's ratio, dynamic strength, and elastic wave velocity are important factors for describing the dynamic properties of rock mass, and ultrasonic wave testing is effective in the field for its convenience. However, the instinct relationship between the ultrasonic wave testing results and mechanical testing results are not quite clear yet and therefore, this study investigates this relationship.

The relationship between P-wave velocity V_P and S-wave velocity V_S with elastic parameters of rock mass is deduced by Feng (1988) and can be expressed as

$$\begin{cases} V_P = \sqrt{\dfrac{E_d(1-\nu)}{\rho(1+\nu)(1-2\nu)}}, \\ V_S = \sqrt{\dfrac{\mu}{\rho}} = \sqrt{\dfrac{E_d}{2\rho(1+\nu)}}, \end{cases} \tag{1}$$

$$\begin{cases} E_d = \dfrac{\rho V_S^2(3V_P^2 - 4V_S^2)}{V_P^2 - V_S^2}, \\ \mu = \rho V_S^2, \\ \nu = \dfrac{V_P^2 - 2V_S^2}{2(V_P^2 - V_S^2)}, \end{cases} \tag{2}$$

where E is the elastic modulus; μ is the shear modulus; and ν is Poisson's ratio. The subscripts d and s denote dynamic and static, respectively. Density ρ reflects the composition of rock mass. Static and dynamic mechanical properties are closely related to the composition of rock mass, and therefore the quality of rock mass can be evaluated by determining and comparing both of these two mechanical properties.

In the project of the Xishan Rock Cliff Statue protection, rock samples were collected from two horizontal drilling holes for ultrasonic acoustic testing and mechanical testing to determine the density of the rock, static elastic modulus, static Poisson's ratio, uniaxial compressive strength and elastic wave velocity. Dynamic elastic modulus of rock and dynamic Poisson's ratio were calculated. Furthermore, the intrinsic relationship between the densities of the rock samples with static and dynamic mechanical parameters were analyzed. The relationship between spatial variations of rock quality with engineering geological conditions and the boundary conditions of rock were revealed, providing a basis of reinforcement for the rock cliff statue.

DSG ultrasonic exploration setup was applied for the testing, as shown in Fig. 1. The frequency range was 10 Hz–2.5 MHz. Firstly, the receiver probe was attached into one end of the rock specimen. Then, an impulse force was excited in the other end of the rock specimen. The wave was recorded by the computer. The diameter of the specimens is 50 mm and the height is 100 mm. The time-travelling method was used for the analysis. Fig 2 illustrates the flow chart of the testing procedure.

Fig. 1 DSG-X ultrasonic test setup

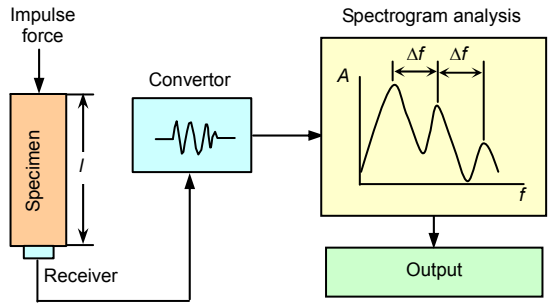

Fig. 2 Flow chart of the wave velocity measurement of rock specimens
l: specimen length; *A*: wave amplitude; *f*: frequency

INSTRON 1346 Servo-control Testing System was applied for the compressive strength testing of the rock specimens. The force increase rate was 0.8 MP/s. CSS-84 Servo-control Testing System was applied for tensile strength testing for the rock specimens. The force increase rate was 0.2 MPa/s. The force was increased gradually until failure. The rock specimen was positioned in the centre of end plates before applying force. The geometrical size of the tensile testing specimen was approximately 50 mm (diameter)×100 mm (height).

3 Xishan Rock Cliff Statue

The Xishan Rock Cliff Statue is approximately 1 km away from Shidi village of Jinyuan District in Taiyuan, China. The geographical coordinates of the statue are 112°11′11″ N, 37°48′33″ E. The elevation of the statues ranges from 850 to 900 m. It is located on hilly areas and joints in rock mass exist in large quantities as a result of terrain faults. The cliff statue belongs in a great tectonic erosion area. The cliff statue faces south. It was carved in the North Qi empire (551–576 AD), a kingdom in Chinese history. It is nearly 1400 years and was produced 227 years earlier than Leshan Giant Buddha Statue, Sichuan, China. The head of the statue was seriously damaged and dropped off in 1363 AD according to history recorded by No. 3 Brigade of Hydrogeology and Engineering Geology under Geology and Mineral Bureau of Shanxi Province (1973).

The bottom of the cliff statue was covered by fragmentized rock and other sediments since then so that the Xishan Rock Cliff Statue was obliterated after nearly 640 years. In 1980, the statue was rediscovered and in 1983, archaeological investigation was undertaken then it reappeared to the public (Du, 2001). It has been 30 years since the rediscovery of the cliff statue and excavation and the weathering is quite serious. Measurement in the field shows that the height from the neck of the Buddha statue to the bottom is rough 30 m and the width of statue is close to 25 m. Until now, it is the oldest Buddha rock statue known in the world.

The Xishan Rock Buddha Statue is mainly constituted of sandstone. The rock mass from the shoulder to the chest is composed of sandwich sandstone. In the abdomen part of the statue, a thin sheet of fractured argillaceous fine-grained sandstone exists. In this area, many parts of the statue surface dropped off as a result of long-time weathering and other man-made damage and a slight groove formed as a consequence of the weathering effect. To study the quality change of rock mass along depth of the statue, two horizontal holes, located east of a groove outside of the statue, were drilled with spacing of 1 m. Both holes were drilled to a depth of 10 m. The rock specimens were retrieved at different depths. Fig. 3 shows the full-face appearance of the rock status. Fig. 4 shows the depths where rock specimens were obtained. Fig. 5 illustrates the lithology of the cliff statue. The two horizontal holes were drilled with an

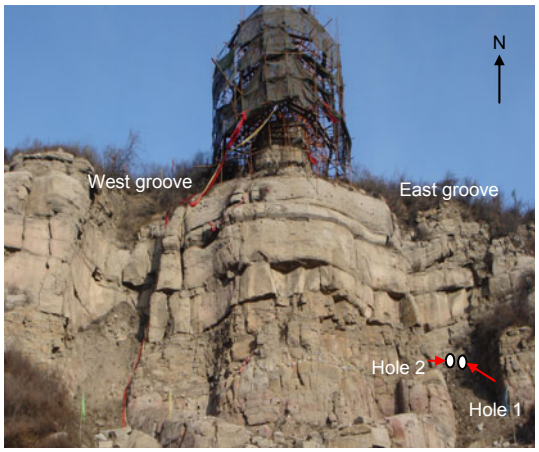

Fig. 3 Main body of the Xishan Rock Buddha Statue

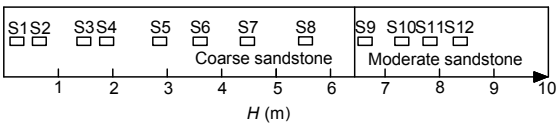

Fig. 4 The position of the specimens
S1–S12: specimen, *H*: hole depth

elevation of 478 m. Fig. 6 shows the engineering geological map of the Xishan Rock Cliff Statue.

4 Spatial distribution of static and dynamic parameters

4.1 Block density and its distribution

The bulk density of rock samples is one of the main parameters that can reflect the physical state of rock mass. Table 1 gives the description of the specimens' lithology of two horizontal holes. The test results of rock dry density are listed in Table 2. The relationship between density and drilling depth is illustrated in Fig. 7 (p.777). It is shown that the bulk density of the specimens in Hole 1 is slightly larger than that in Hole 2. The densities of the specimens obtained in Holes 1 and 2 centralize in the ranges of 2.3–2.5 and 2.1–2.3 g/cm^3, respectively. This phenomenon is closely related to the hole positions. Hole 2 is closer to the east groove area of fractured argillaceous fine-grained sandstone. Therefore, the rock mass near Hole 2 suffered more unloading effect and weathering. The rock mass near Hole 2 is looser.

On the whole, the bulk density increases with augmentation of the horizontal depth H. This increase rate reduces gradually when the hole depth increases. The density change tendency in hole depth shows that the weathering degree in the statue surface is much more serious than the inner rock mass. When the depth is in the range of 2.5 to 3.0 m, the density increases rather quick and it shows that the degree is quite diverse in this depth zone and the quality of rock mass improves much when the depth increases. When the depth is larger than 3.0 m, the increasing speed of density reduces to a stable value reflecting that

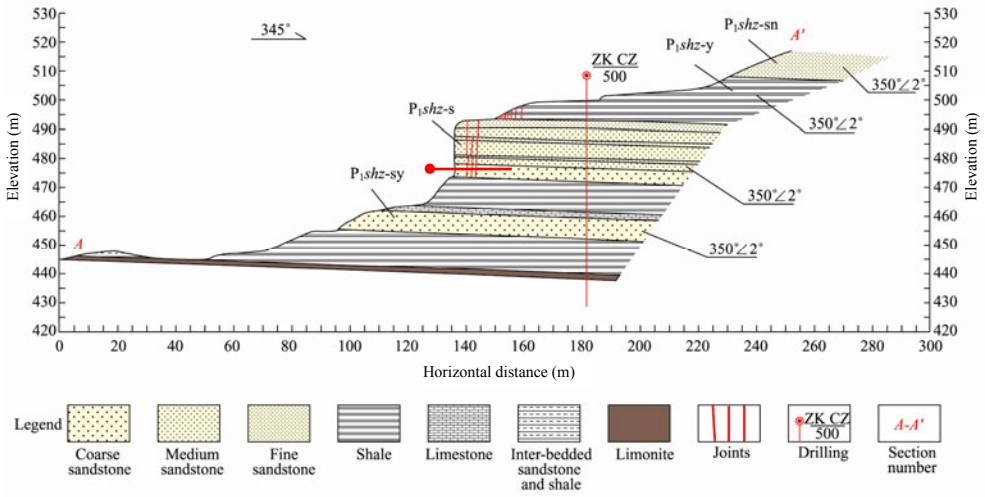

P_1shz-sn: sandstone and mudstone of Shihezi formation of lower series in Permian; P_1shz-y: shale of Shihezi formation of lower series in Permian; P_1shz-s: sandstone of Shihezi formation of lower series in Permian; P_1shz-sy: blending of sandstone and shale of Shihezi formation of lower series in Permian

Fig. 5 Cross section A–A of the Xishan Rock Cliff Statues

Table 1 Description of the lithology of the specimens in two horizontal holes

Hole No.	H (m)	Lithology description
1	2.2	Coarse sandstone, joints exist, rock is loose
	4.4	Coarse sandstone, with some limestone, rock block is dense
	6.2	Coarse sandstone, with some limestone, rock block is dense
	7.6	Moderate sandstone, the main component is quartz, rock block is dense
	9.0	Moderate sandstone, the main component is quartz, rock block is dense
2	2.3	Coarse sandstone, with some limestone, joints exist, rock is loose
	4.5	Coarse sandstone, joints exist, rock is loose, with some limestone
	6.5	Coarse sandstone, joints exist, rock is loose, with some limestone
	8.8	Moderate sandstone, the main component is quartz, joints exist, rock is loose

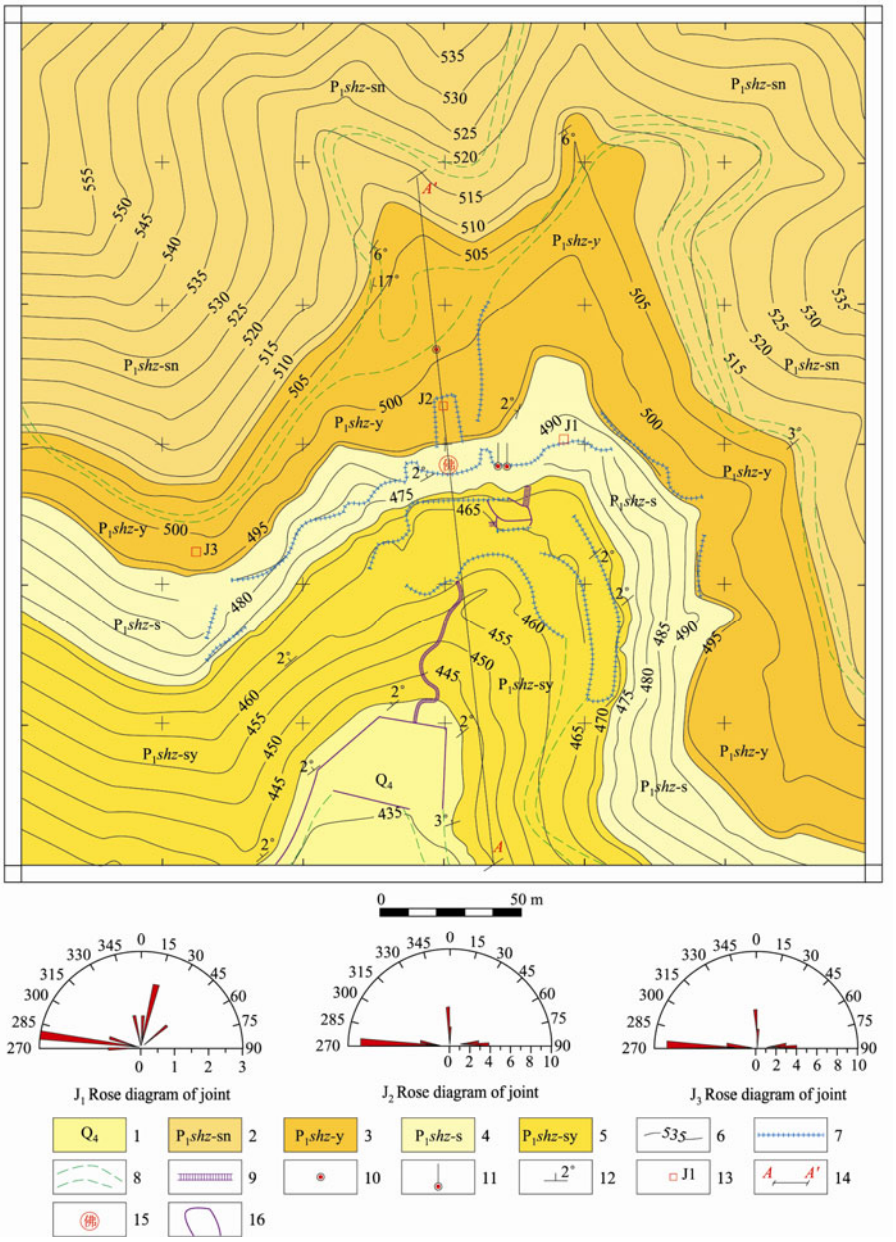

1: holocene series; 2: sandstone and mudstone of Shihezi formation of lower series in Permian; 3: shale of Shihezi formation of lower series in Permian; 4: sandstone of Shihezi formation of lower series in Permian; 5: blending of sandstone and shale of Shihezi formation of lower series in Permian; 6: contour line of landform; 7: cliff; 8: path; 9: steps; 10: vertical drilling; 11: horizontal drilling; 12: attitude of strata; 13: statistic point of joints; 14: section line; 15: position of Buddha; 16: platform

Fig. 6 Engineering geological map of the Xishan rock cliff statues

Table 2 Distribution of bulk density of specimens in two horizontal holes

H (m)	ρ (g/cm^3)		Lithology	H (m)	ρ (g/cm^3)		Lithology
	Hole 1	Hole 2			Hole 1	Hole 2	
0.40	2.27	2.13	Coarse sandstone	4.60	2.37	2.24	Coarse sandstone
0.80	2.45	2.15	Coarse sandstone	5.60	2.44	2.27	Coarse sandstone
1.50	2.33	2.11	Coarse sandstone	6.40	2.45	2.31	Coarse sandstone
2.00	2.45	2.18	Coarse sandstone	7.20	2.45	2.26	Moderate sandstone
3.00	2.46	2.20	Coarse sandstone	7.90	2.44	2.29	Moderate sandstone
3.70	2.38	2.22	Coarse sandstone	8.30	2.50	2.36	Moderate sandstone

the quality of rock mass does not change much and the composition and structure difference of the rock mass do not vary greatly.

4.2 Dynamic parameters and distribution

From Eq. (1), it can be seen that the velocities of elastic wave V_P and V_S are dependent on the density of rock, elastic modulus and Poisson's ratio. Therefore, the elastic wave velocity can reflect the mechanical properties of rock mass effectively. Table 3 and Table 4 show the ultrasonic wave testing results of the specimens retrieved in Hole 1 and Hole 2, respectively. The dynamic elastic modulus E_d and dynamic Poisson's ratio ν_d is calculated according to Eq. (2). From Fig. 8, it can be seen that, in general, P-wave velocity V_P in the specimen of Hole 1 is slightly higher than that of Hole 2, though in some specimens, the test value appears scattered. With an increase of

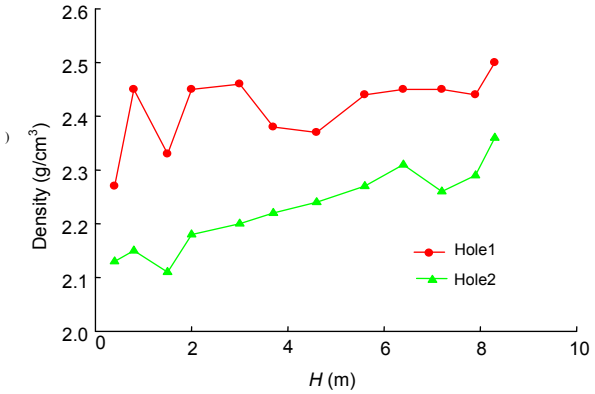

Fig. 7 Relationship between the bulk densities of rock specimens and hole depth

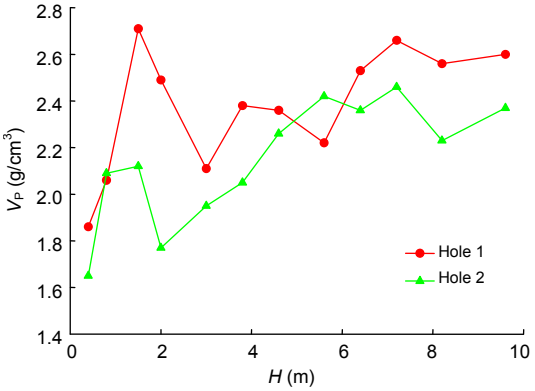

Fig. 8 Relationship between the wave velocity and hole depth

Table 3 Results of ultrasonic wave testing on rock specimens of Hole 1

Specimen No.	H (m)	V_P (km/s)	V_S (km/s)	E_d (GPa)	ν_d
1	0.4	1.86	1.18	7.35	0.16
2	0.8	2.06	1.25	9.25	0.21
3	1.5	2.71	1.34	11.20	0.34
4	2.0	2.49	1.25	10.19	0.33
5	3.0	2.11	1.21	9.04	0.26
6	3.8	2.38	1.39	11.41	0.24
7	4.6	2.36	0.98	6.35	0.40
8	5.6	2.22	1.24	9.55	0.27
9	6.4	2.53	1.29	10.80	0.32
10	7.2	2.66	1.35	11.85	0.33
11	8.2	2.56	1.37	11.90	0.30
12	9.6	2.60	1.37	12.27	0.31

Table 4 Results of ultrasonic wave testing on rock specimens of Hole 2

Specimen No.	H (m)	V_P (km/s)	V_S (km/s)	E_d (GPa)	ν_d
1	0.4	1.65	1.05	5.45	0.16
2	0.8	2.09	1.11	6.91	0.30
3	1.5	2.12	1.19	7.59	0.27
4	2.0	1.77	1.00	5.52	0.27
5	3.0	1.95	1.14	7.09	0.24
6	3.7	2.05	1.25	8.35	0.20
7	4.6	2.26	1.27	9.17	0.27
8	5.6	2.42	1.41	11.22	0.24
9	6.4	2.36	1.12	7.85	0.35
10	7.2	2.46	1.32	10.22	0.30
11	7.9	2.23	0.87	4.89	0.41
12	8.3	2.37	1.35	10.84	0.26

hole depth, the wave velocity in the two holes rises. From Fig. 9, where the relationship between dynamic elastic modulus of the specimen with hole depth is illustrated, the dynamic elastic modulus in the specimen of Hole 1 is slightly higher than Hole 2. This trend coincides with the density variation tendency along the hole depth.

4.3 Static parameters and distribution

To understand the static mechanical performance of rock specimens, uniaxial compression tests and tensile strength testing for the specimens drilled from Hole 1 are undertaken in saturation. Table 5 lists the detailed test values. Fig. 10 shows the relationship between compression strength in saturation σ_c and tensile strength σ_t with hole depth. It shows a similar variation tendency in depth with density. It seems that rock uniaxial compressive strength is more scattered when compared with tensile strength. The phenomenon may be caused by low capacity of tensile strength of the rock which means that whether there are cracks in the rock or not, the tensile strengths gather in a low area (less than 5 MPa). The density, composition and environmental form have more influence on the uniaxial compressive strength.

4.4 Comparison between static and dynamic parameters

Fig. 11 illustrates the comparison between dynamic elastic modulus E_d and static elastic modulus E_s. The variation tendency of elastic modulus with increase of hole depth shows that both E_d and E_s increase with augmentation of the hole depth. At the same time, the increasing speed of these two values along hole depth becomes slower and slower with increase of hole depth. In most specimens, the dynamic elastic modulus E_d locates in the range of 8.0 to 15.0 GPa and the static elastic modulus E_s ranges from 2.2 to 3.2 GPa. It can be found that E_d and E_s have different distribution areas. However, both the values show a similar variation tendency. Additionally, the dynamic modulus E_d fluctuates more easily than the static modulus E_s because of crack pattern and specimen processing condition.

Fig. 12 shows the relationship between static elastic modulus E_s and P-wave velocity V_P in the

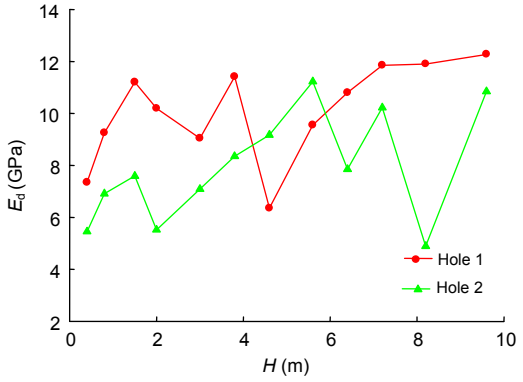

Fig. 9 Relationship between dynamic modulus and hole depth

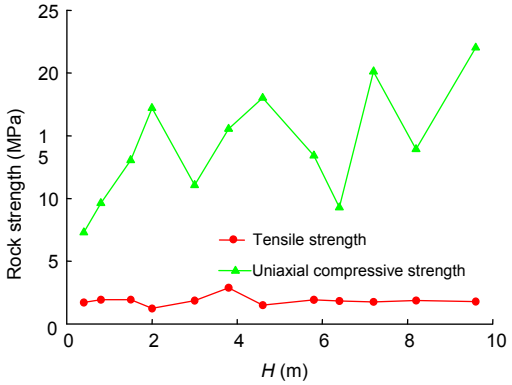

Fig. 10 Relationship between tensile and compressive strengths and hole depth

Table 5 Mechanical testing results of rock specimens drilled in Hole 1

Specimen No	H (m)	σ_t (MPa)	σ_c (MPa)	E_s (GPa)	ν_s
1	0.40	1.72	7.29	3.13	0.13
2	0.80	1.93	9.63	3.17	0.17
3	1.50	1.94	13.05	3.88	0.15
4	2.00	1.24	17.20	4.27	0.23
5	3.00	1.86	11.06	3.32	0.19
6	3.80	2.88	15.54	4.05	0.27
7	4.60	1.50	18.01	3.55	0.26
8	5.80	1.92	13.41	3.75	0.14
9	6.40	1.83	9.28	4.10	0.22
10	7.20	1.76	20.11	4.25	0.43
11	8.20	1.87	13.92	4.46	0.36
12	9.60	1.79	22.01	4.82	0.27

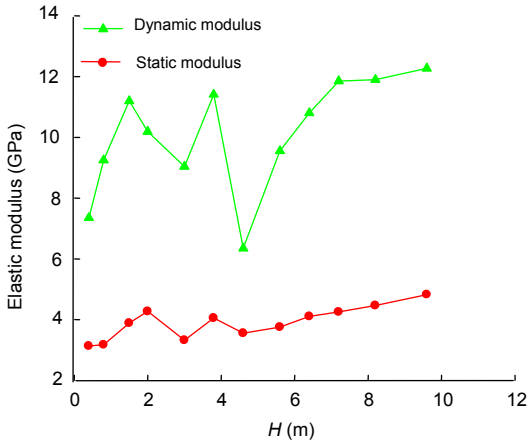

Fig. 11 Comparison between dynamic and static elastic modulus

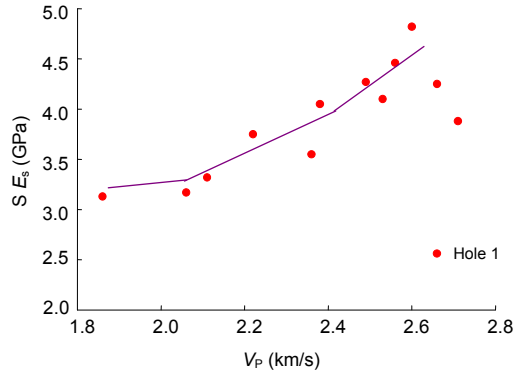

Fig. 12 Relationship between static elastic modulus and P-wave velocity

specimens of Hole 1. In theory, the static modulus E_s should show a positive relationship with elastic wave velocity. However, some points' distribution seems a little scattered though there is an obvious connection between E_s and V_P. The factors causing data anomalies can be discovered in view of physical fabric of the rock specimens. For example, for the point at V_p= 2.71 km/s, E_s=3.83 GPa, as shown in Fig. 13, it is found that the wave velocity is high while the static elastic modulus is quite low and this phenomenon is due to the existence of micro cracks in the specimen along axis direction. Therefore, the wave velocity is not greatly influenced by cracks while the compression capacity of the specimen is greatly reduced. Lateral deformation is enlarged, and therefore axis deformation is also enlarged. For the point at V_P =1.86 km/s, E_s=3.13 GPa, as shown in Fig. 14, it is found that the velocity of P-wave is low and the static elastic modulus is high. It can be found in this specimen that several micro cracks exist approximately along a lateral direction. When P-wave is transmitted through the specimen, it is greatly influenced by these micro cracks and shows reduced transmission velocity. However, compression capacity of the specimen is not greatly influenced by such micro cracks so that the static elastic modulus is high.

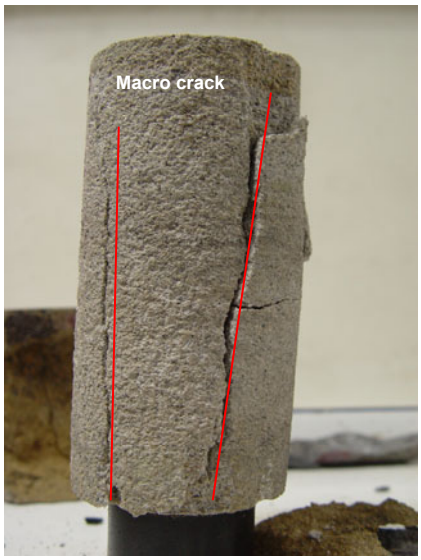

Fig. 13 The specimen with cracks in axis direction

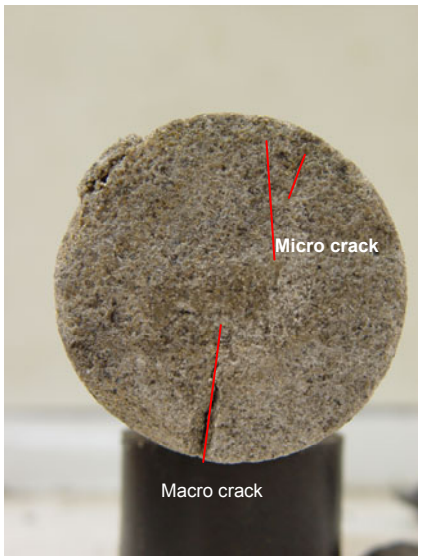

Fig. 14 The specimen with cracks in lateral direction

5 Conclusions

By analyzing mechanical testing data of the specimens in two drilled holes in the Xishan Rock Buddha Statue, some conclusions can be drawn.

1. The density, static parameter and dynamic parameter show a consistent tendency along the depth of drilled holes. These parameters can be used in the evaluation of weathering of rock mass. It can be found that the weathering of rock mass within 2.5 m in depth is quite serious. When the hole depth is larger than 3.0 m, the rock mass is less weathered and the density increases steadily.

2. There are obvious differences in density and dynamic elastic modulus of the two holes. The quality of rock mass near Hole 1 is better than that near Hole 2. This is closely related to the unloading effect in the free border of the rock mass. The mechanical testing results and ultrasonic testing results agree well and both methods can be used in analysis for quality of rock mass and engineering geology condition.

3. The dynamic elastic modulus is more sensitive to the change of rock quality than P-wave velocity. Therefore, the dynamic elastic modulus of rock can reflect the spatial variation of rock mass quality better.

4. The rock fabric has a significant influence on static and dynamic parameters. Micro cracks in an axis direction of the rock specimens can induce abnormal phenomenon showing high P-wave velocity and low static elastic modulus. Micro cracks in a lateral direction of the rock specimens can induce another anomalous phenomenon showing low P-wave velocity and high static elastic modulus. Non-uniformity and micro cracks in rock will lead to abnormality of the corresponding relationship between static and dynamic parameters.

Based on the test results and analysis, it can be concluded that the ultrasonic testing is an efficient method to get rock fabric and dynamic parameters and it is an efficient technique for evaluating weathering degree of cultural rock relics. The test results provide a basis of reinforcement for rock mass stability of the Xishan Rock Buddha Statue.

References

Bhasin, R., Kaynia, A.M., 2004. Static and dynamic simulation of a 700-m high rock slope in western Norway. *Engineering Geology*, **71**(3-4):213-216. [doi:10.1016/S0013-7952(03)00135-2]

Bray, J., Repetto, P.C., 1994. Seismic design consideration for lined solid waste landfills. *Geotextiles and Geomembranes*, **13**(8):497-518. [doi:10.1016/0266-1144(94)90015-9]

Camborde, F., Mariotti, C., Donze, F.V., 2000. Numerical study of rock and concrete behavior by discrete element modeling. *Computers and Geotechnics*, **27**(4):225-247. [doi:10.1016/S0266-352X(00)00013-6]

Deng, T., Han, W.F., Bao, H.Z., 2000. Research of wave diversification characteristic of marbles saturated in water. *Chinese Journal of Rock Mechanics and Engineering*, **19**(6):762-765 (in Chinese).

Du, J.H., 2001. Jinyang Literature and Historical Document (Volume 5). Jinyuan Committee of Literature and Historical under Chinese People's Political Consultative Conference Taiyuan Committee, Taiyuan (in Chinese).

Feng, Y.D., 1988. The Theory and Appliance of Seismic Wave. The Publish Company of Earthquake, Beijing.

Guyer, R.A., McCall, K.R., Boitnott, G.N., 1997. Quantitative implementation of Preisach-Mayergoyz space to find static and dynamic moduli in rock. *Journal of Geophysical Research*, **102**(B3):5281-5293. [doi:10.1029/96JB03740]

Homand, F., Morel, E., Henry, J.P., Cuxac, P., Hammade, E., 1993. Characterization of the moduli of elasticity of an anisotropic rock using dynamic and static methods. *International Journal of Rock Mechanics and Mining Sciences & Geomechanics Abstracts*, **30**(5):527-535. [doi:10.1016/0148-9062(93)92218-F]

Jiang, J., 2008. Dynamic Stability Analysis of the Xishan Buddha Rock Slope under Condition of Earthquake. MS Thesis, China University of Geosciences, Beijing (in Chinese).

Khan, A.S., Irani, F.K., 1987. An experimental study of stress wave transmission at a metallic-rock interface and dynamic tensile failure of sandstone, limestone, and granite. *Mechanics of Materials*, **6**(4):285-292.

Li, H.B., Wu, M.B., 1995. Sonic wave testing and research of rock mass in the area of Longmen grotto. *Soil and Rock Mechanics*, **16**(3):443-481.

Ling, H.I., Cheng, A.H.D., 1997. Rock sliding induced by seismic force. *International Journal of Rock Mechanics and Mining Science*, **34**(6):1021-1029. [doi:10.1016/S1365-1609(97)80011-1]

Mao, J.H., Li, S.L., Wang, N., 2005. The application and research of sonic wave measuring and sonic transmission in the rock mass. *China Colour Metal Transaction*, **8**(Supp. II):758-762 (in Chinese).

No. 3 Brigade of Hydrogeology and Engineering Geology under Geology and Mineral Bureau of Shanxi Province, 1973. Introduction of Engineering Geology Map of Taiyuan, People's Republic of China (1:100 000). National Geology Archive, Beijing.

Ravazzoli, C.L., Santos, J.E., Carcione, J.M., 2003. Acoustic and mechanical response of reservoir rocks under variable saturation and effective pressure. *Journal of the*

Acoustical Society of America, **113**(4):1801-1811. [doi:10.1121/1.1554696]

Sun, J.Z., 2001. The Research on Some Application Problems of Dynamics of Rock and Soil Mass. PhD Thesis, China University of Geosciences, Beijing (in Chinese).

Wiercigroch, M., Wojewoda, J., Krivtsov, A.M., 2005. Dynamics of ultrasonic percussive drilling of hard rocks. *Journal of Sound and Vibration*, **280**(3-5):739-757. [doi:10.1016/j.jsv.2003.12.045]

Xu, B.T., Wang, H.X., 2004. Contrast testing study on dynamic rock mass parameters by different dynamic method. *Chinese Journal of Rock Mechanics and Engineering*, **23**(2):284-288 (in Chinese).

Zhao, M.J., 1999. Research of acoustic characteristic of cranny rock mass in the condition of load. *Chinese Journal of Rock Mechanics and Engineering*, **18**(2):240 (in Chinese).

Zhou, X.M., Shen, Q., Xiong, S.H., 2002. Value-choosing research of parameter of complicated rock mechanics. *Chinese Journal of Rock Mechanics and Engineering*, **21**(Supp.):2045-2048 (in Chinese).

Zhu, H.C., 1999. Sonic wave measuring and analysis of high rock slope. *Chinese Journal of Rock Mechanics and Engineering*, **18**(4):378-381 (in Chinese).